

Efficient wave propagation on complex domains

By K. Mattsson, F. Ham AND G. Iaccarino

1. Motivation and objectives

In many applications, such as general relativity (see, for example, Szilagyl *et al.* (2005)), seismology, and acoustics, the underlying equations are systems of second-order hyperbolic partial differential equations. However, as pointed out by Kreiss *et al.* (2002), with very few exceptions (see for example Kreiss *et al.* (2002, 2004); Shubin & Bell (1987); Bamberger *et al.* (1997); Cohen & Joly (1996)), the equations are rewritten and solved on first-order form. There are three obvious drawbacks with this approach: 1) the number of unknowns is doubled, 2) spurious oscillations due to unresolved features might be introduced, and 3) double resolution (both in time and in each of the spatial dimensions) is required to obtain the same accuracy. The reasons for solving the equations in first-order form are due to the fact that computational methods for first-order hyperbolic systems are very well developed, and they are naturally more suited for complex geometries.

For problems on complex domains it is very difficult to maintain both high-order accuracy and efficiency. To retain high-order accuracy for problems with discontinuities in the coefficients is another concern (see for example Gustafsson & Mossberg (2004) and Gustafsson & Wahlund (2004)). High-order finite difference methods are very accurate and efficient on problems that are relatively simple geometrically. In Mattsson & Nordström (2006) high-order accurate, strictly stable schemes for the wave equations on discontinuous media were constructed by combining compact Summation-By-Parts (SBP) operators (constructed in Mattsson & Nordström (2004)) with the projection method. However, on complex domains it is difficult to obtain a high quality grid that supports high-order accuracy. In Kreiss *et al.* (2002, 2004, 2006) a second-order accurate finite difference method for the wave equation on second-order form was constructed, where the geometry is handled by embedding the domain into a Cartesian grid. It is unclear if that technique can be extended to accurately handle discontinuous media.

In this paper we will show how to impose boundary and discontinuous interface conditions in a strictly stable way by combining compact second derivative SBP operators and the Simultaneous Approximation Term (SAT) method by Carpenter *et al.* (1994). To handle complex geometries we will make use of a compact and second-order accurate Laplacian operator with SBP property on unstructured grids (presented in Ham *et al.* (2006) elsewhere in this volume).

In Section 2 we introduce some definitions and discuss the SBP property for the second derivative. In Section 3 we introduce the numerical method by considering the second-order wave equation in one dimension (1-D). In Section 4 we verify the accuracy and stability properties by performing numerical computations on complex geometries using an unstructured finite volume discretization. In Section 5 we present our conclusions.

2. Definitions

Definitions are needed to describe the SBP property in detail. For clarity we consider the 1-D problem. The extension to the 3-D unstructured case is directly related to the 1-D analysis through the use of matrix notation, as will be shown in Section 4.

2.1. The energy method

Let the inner product for real valued functions $u, v \in \mathbf{L}^2[0, 1]$ be defined by $(u, v) = \int_0^1 u^T v \, dx$, and let the corresponding norm be $\|u\|^2 = (u, u)$. We also introduce a weighted norm

$$\|u\|_\omega^2 = \int_0^1 u^T u \omega(x) \, dx,$$

where $\omega(x) \in \mathbf{L}^2[0, 1]$ is a positive function. The domain $(0 \leq x \leq 1)$ is discretized using $N+1$ equidistant grid points,

$$x_i = i h, \quad i = 0, 1, \dots, N, \quad h = \frac{1}{N}.$$

The numerical approximation at grid point x_i is denoted v_i , and the discrete solution vector is $v^T = [v_0, v_1, \dots, v_N]$. We define an inner product for discrete, real valued vector-functions $u, v \in \mathbf{R}^{N+1}$ by $(u, v)_H = u^T H v$, where $H = H^T > 0$, with a corresponding norm $\|v\|_H^2 = v^T H v$.

2.2. Summation-By-Parts property

An SBP operator mimics the behavior of the corresponding continuous operator with respect to the inner product previously mentioned. Consider the wave equation $au_{tt} = (bu_x)_x$, $x \in [0, 1]$, and $a, b > 0$. Integration by parts (IBP) leads to

$$\frac{d}{dt} (\|u_t\|_a^2 + \|u_x\|_b^2) = 2buu_x|_0^1. \quad (2.1)$$

Consider the semi-discrete approximation $AHv_{tt} = (-M + BS)v$, where A is the projection of a onto the diagonal. By multiplying the semi discrete approximation by v_t^T and by adding the transpose, we obtain

$$\frac{d}{dt} (\|v_t\|_{HA}^2 + v^T M v) = 2v_0(BSv)_0 + 2v_N(BSv)_N. \quad (2.2)$$

To obtain (2.2) requires that 1) $H > 0$ and diagonal, 2) $M = M^T \geq 0$, and 3) BS mimic the boundary derivative operator. Formula (2.2) is a discrete analog to the IBP formula (2.1) in the continuous case. The above procedure is referred to as the energy method. We introduce the following definition:

DEFINITION 2.1. *A difference operator $D_2 = H^{-1}(-M + BS)$ approximating $(bu_x)_x$ is said to be a symmetric second derivative SBP operator if H is diagonal and positive definite, M is symmetric and positive semi-definite, S includes an approximation of the first derivative operator at the boundary, and $B = \text{diag}(-b_0, 0, \dots, 0, b_N)$.*

3. Boundary treatment

In this method developed by Carpenter *et al.* (1994), the boundary conditions are introduced as a penalty term. When the energy method is applied, a discrete analog to the continuous energy is obtained.

Consider the 1-D wave equation on second-order form:

$$\begin{aligned} au_{tt} &= (bu_x)_x + F, \quad 1 \geq x \geq 0, \quad t \geq 0 \\ u &= f_1, \quad u_t = f_2, \quad 1 \geq x \geq 0, \quad t = 0, \end{aligned} \quad (3.1)$$

where $\sqrt{a^{-1}b} = c$ is the wave speed. For density waves $a^{-1} = \rho c^2$, and $b^{-1} = \rho$, where $\rho > 0$ is the density of the media. General boundary conditions are given by

$$\begin{aligned} L_l u &= \beta_1 u(0, t) - \beta_2 b_0 u_x(0, t) + \beta_3 u_t(0, t) = g_l(t) \\ L_r u &= \beta_1 u(1, t) + \beta_2 b_N u_x(1, t) + \beta_3 u_t(1, t) = g_r(t) \end{aligned} \quad (3.2)$$

Note that (3.2) includes the special case of Dirichlet boundary conditions (and radiation boundary conditions. See for example Tsynkov (1998) and Hagstrom (1999)).

3.1. Mixed boundary conditions

We start by considering the case where $\beta_2 \neq 0$, which includes the important case of Neumann boundary conditions ($\beta_1 = 0$, $\beta_2 = 1$, $\beta_3 = 0$). Assuming zero boundary data and forcing function F , the energy method leads to

$$\frac{d}{dt} \left(\|u_t\|_a^2 + \|u_x\|_b^2 + \frac{\beta_1}{\beta_2} u_0^2 + \frac{\beta_1}{\beta_2} u_1^2 \right) = -\frac{\beta_3}{\beta_2} (u_t^2)_0 - \frac{\beta_3}{\beta_2} (u_t^2)_1. \quad (3.3)$$

Hence, the continuous problem (3.1) and (3.2) have an energy estimate if

$$\frac{\beta_1}{\beta_2} \geq 0, \quad \frac{\beta_3}{\beta_2} \geq 0. \quad (3.4)$$

The semi-discrete boundary conditions corresponding to (3.2) can be written

$$\begin{aligned} L_l^T v &= \beta_1 v_0 + \beta_2 (BSv)_0 + \beta_3 (v_t)_0 = g_l \\ L_r^T v &= \beta_1 v_N + \beta_2 (BSv)_N + \beta_3 (v_t)_N = g_r, \end{aligned} \quad (3.5)$$

where v is the discrete solution vector, S is the boundary derivative operator in Definition 2.1, and $B = \text{diag}(-b_0, 0 \dots, 0, b_N)$.

The SAT method for the wave equation in second-order form with the boundary conditions (3.2), can be written

$$\begin{aligned} HAv_{tt} &= (-M + BS)v + \tau e_0 (L_l^T v - g_l) + \tau e_N (L_r^T v - g_r) + F \\ v &= f_1, \quad v_t = f_2, \quad t = 0. \end{aligned} \quad (3.6)$$

LEMMA 3.1. (3.6) with homogenous data has a non-growing solution if D_2 is a symmetric SBP operator, $\tau = 1/\beta_2$ and (3.4) hold.

Proof. Let $F, g_l, g_r = 0$. Multiplying (3.6) by v_t^T from the left and adding the transpose leads to

$$\begin{aligned} v_t^T HAv_{tt} + v_{tt}^T HAv_t &= -v_t^T Mv - v^T M^T v_t + 2(v_t)_0 (BSv)_0 + 2(v_t)_N (BSv)_N \\ &\quad + 2\tau (v_t)_0 (\beta_1 v_1 + \beta_2 (BSv)_0 + \beta_3 (v_t)_0) \\ &\quad + 2\tau (v_t)_N (\beta_1 v_N + \beta_2 (BSv)_N + \beta_3 (v_t)_N) \end{aligned} \quad .$$

If D_2 is a symmetric SBP, operator we obtain

$$\begin{aligned} \frac{d}{dt} \left(\|v_t\|_{H_A}^2 + v^T Mv - \tau \beta_1 v_0^2 - \tau \beta_1 v_N^2 \right) &= +\tau \beta_3 (v_t)_0^2 + \tau \beta_3 (v_t)_N^2 \\ &\quad + 2(1 + \tau \beta_2) (v_t)_0 (BSv)_0 + 2(1 + \tau \beta_2) (v_t)_N (BSv)_N \end{aligned} \quad .$$

If $\tau = -1/\beta_2$, we obtain an energy estimate completely analogous to (3.3). If (3.4) holds, we have a non-growing energy. \square

3.2. Dirichlet boundary conditions

We now consider the case of Dirichlet boundary conditions ($\beta_1 = 1$, $\beta_2 = 0$, $\beta_3 = 0$). We introduce the following Lemma:

LEMMA 3.2. *The dissipative part M of a symmetric second-derivative SBP operator has the following property:*

$$v^T M v = h \frac{\alpha}{b_0} (BSv)_0^2 + h \frac{\alpha}{b_N} (BSv)_N^2 + v^T \tilde{M} v, \quad (3.7)$$

where \tilde{M} is symmetric and positive semi-definite, and α a positive constant, independent of h .

This was indicated in Carpenter *et al.* (1999) but never derived explicitly. With Dirichlet boundary condition ($\beta_1 = 1$, $\beta_2 = 0$, $\beta_3 = 0$) and homogenous data, the energy method leads to

$$\frac{d}{dt} (\|u_t\|_a^2 + \|u_x\|_b^2) = 0. \quad (3.8)$$

The SAT method for the wave equation on second-order form and Dirichlet boundary conditions is given by

$$\begin{aligned} H A v_{tt} &= (-M + BS)v + \epsilon (BS)^T e_0 (v_0 - g_l) + \sigma b_0 e_0 (v_0 - g_l) + F \\ &\quad + \epsilon (BS)^T e_N (v_N - g_r) + \sigma b_N e_N (v_N - g_r) \\ v(0) &= f_1, \quad v_t(0) = f_2. \end{aligned} \quad (3.9)$$

LEMMA 3.3. *(3.9) with homogenous data has a non-growing solution if D_2 is a symmetric SBP operator, $\sigma \leq -\frac{1}{\alpha h}$, $\epsilon = 1$, and (3.7) hold.*

Proof. Let $F, g_l, g_r = 0$. Multiplying (3.9) by v_t^T from the left and adding the transpose leads to

$$\begin{aligned} v_t^T H A v_{tt} + v_{tt}^T A H v_t &= -v_t^T M v - v^T M^T v_t + 2(v_t)_0 (BSv)_0 + 2(v_t)_N (BSv)_N \\ &\quad + 2\epsilon (BSv_t)_0 v_0 + 2\sigma b_0 (v_t)_0 v_0 \\ &\quad + 2\epsilon (BSv_t)_N v_N + 2\sigma b_N (v_t)_N v_N \end{aligned}$$

If D_2 is a symmetric SBP operator, $\epsilon = 1$ and (3.7) hold, we obtain

$$\frac{d}{dt} \left(\|v_t\|_{H A}^2 + v^T \tilde{M} v + w_0^T R_0 w_0 + w_N^T R_N w_N \right) = 0,$$

where $w_{0,N}^T = [v_{0,N}, (BSv)_{0,N}]$ and

$$R_0 = \begin{bmatrix} -\sigma b_0 & -1 \\ -1 & \frac{\alpha h}{b_0} \end{bmatrix}, \quad R_N = \begin{bmatrix} -\sigma b_N & -1 \\ -1 & \frac{\alpha h}{b_N} \end{bmatrix}.$$

Finally, if $\sigma \leq -\frac{1}{\alpha h}$ holds, we have a non-growing energy. \square

We introduce the penalty-strength parameter γ through

$$\sigma = -\gamma \frac{1}{\alpha h}$$

Hence a value of $\gamma < 1$, according to Lemma 3.3, will not result in an energy estimate and might lead to an unstable scheme.

3.3. Discontinuous media interface

We start by deriving the interface conditions for the continuous problem. Consider the wave equation

$$aw_{tt} = (bw_x)_x, \quad x \in [-1, 1], \quad t \geq 0,$$

where $a, b > 0$ are discontinuous at $x = 0$ and $c = \sqrt{b/a}$ is the wave propagation speed. Integration by parts leads to

$$\begin{aligned} \int_{-1}^1 aw_{tt}w_t dx &= \lim_{\epsilon \rightarrow 0} \left(\int_{-1}^{-\epsilon} (bw_x)_x w_t dx - \int_1^{\epsilon} (bw_x)_x w_t dx \right) \\ &= \lim_{\epsilon \rightarrow 0} \left(bw_x w_t|_{-1}^1 - bw_x w_t|_{-\epsilon}^{\epsilon} - \int_{-1}^{-\epsilon} bw_x w_{xt} dx + \int_1^{\epsilon} bw_x w_{xt} dx \right). \end{aligned}$$

Obtaining an energy estimate requires that w and bw_x are continuous across the interface, i.e., $\lim_{\epsilon \rightarrow 0} (bw_x w_t|_{-\epsilon}^{\epsilon}) = 0$, leading to $\frac{d}{dt} (\|w_t\|_a^2 + \|w_x\|_b^2) = bw_x w_t|_{-1}^1$. We consider the following problem

$$\begin{aligned} a_1 u_{tt} &= (b_1 u_x)_x, & -1 \leq x \leq 0 \\ a_2 v_{tt} &= (b_2 v_x)_x, & 0 \leq x \leq 1 \end{aligned}, \quad (3.10)$$

where $a_1 \neq a_2, b_1 \neq b_2$. Continuity at the interface ($x = 0$) means that

$$u_t = v_t, \quad b_1 u_x = b_2 v_x. \quad (3.11)$$

The first condition ($u_t = v_t$) holds if we impose $u = v$ at the interface. This will have implications for the time discretization. The discrete approximation to (3.11) is given by

$$u_N = v_0, \quad (u_t)_N = (v_t)_0, \quad (B_1 S v)_N = (B_2 S v)_0, \quad (3.12)$$

where all conditions (also $u = v$) are written out. If we use the interface conditions (3.11) and apply homogeneous Neumann conditions ($u_x = 0$) at the outer boundaries the energy method leads to

$$\frac{d}{dt} E = 0, \quad (3.13)$$

where the energy is defined as

$$E = \|u_t\|_{a_1}^2 + \|v_t\|_{a_2}^2 + \|u_x\|_{b_1}^2 + \|v_x\|_{b_2}^2. \quad (3.14)$$

We will treat the semi-discrete problem in such a way that we exactly mimic (3.13).

The SAT method for this particular problem (3.10)-(3.11) can formally be written

$$\begin{aligned} HA_1 u_{tt} &= (-M_1 + B_1 S)u & HA_2 v_{tt} &= (-M_2 + B_2 S)v \\ &+ \tau e_N (u_N - v_0) & &+ \tau e_0 (v_0 - u_N) \\ &+ \beta (B_1 S)_N^T e_N (u_N - v_0) & &+ \beta (B_2 S)_0^T e_0 (v_0 - u_N) \\ &+ \gamma e_N ((B_1 S u)_N + (B_2 S v)_0) & &+ \gamma e_0 ((B_2 S v)_0 - (B_1 S u)_N) \\ &+ \sigma e_N ((u_t)_N - (v_t)_0) & &+ \sigma e_0 ((v_t)_0 - (u_t)_N) \\ &+ SAT_l & &+ SAT_r \end{aligned} \quad (3.15)$$

utilizing the discrete conditions (3.12). Here u and v are the solution vectors corresponding to the left and right domain respectively. $SAT_{l,r}$ correspond to the outer boundaries (described in previous sections). The left and right domain is discretized using $(N+1)$ and $(M+1)$ grid points.

We can have different discretizations in the left and right domains. The only requirement for the stability analysis to hold is that we use symmetric SBP operators (see Definition 2.1) in each of the domains.

If we multiply (3.15) by $u_t^T H$ and $v_t^T H$, respectively, we obtain

$$\frac{d}{dt} E_H = 2\sigma v_t^T D v_t, \quad (3.16)$$

where the discrete energy is defined as

$$E_H = \|u_t\|_{HA_1}^2 + \|v_t\|_{HA_2}^2 + u^T M_1 u + v^T M_2 v + IT + BT,$$

where IT corresponds to the interface terms, BT the boundary terms, and

$$D = \begin{bmatrix} 1 & -1 \\ -1 & 1 \end{bmatrix}$$

is a positive semi-definite matrix. The first stability requirement is that $\sigma \leq 0$.

The advantage of choosing $\sigma = 0$ is that we can obtain a compact time discretization. This is also the choice in the computations. However, by choosing $\sigma < 0$ we introduce damping, which will potentially lead to a more robust and less reflective interface treatment. We have not included that numerical study in this paper.

To have a discrete energy we must further show that E_H is positive. Certain relations need to be met to demonstrate this. We begin by recognizing the symmetry conditions

$$\gamma = -\frac{1}{2}, \quad \beta = \frac{1}{2}. \quad (3.17)$$

The interface term is given by $IT = w^T R w$, where

$$R = \begin{bmatrix} -\tau & \tau & -\frac{1}{2} & \frac{1}{2} \\ \tau & -\tau & \frac{1}{2} & -\frac{1}{2} \\ -\frac{1}{2} & \frac{1}{2} & \frac{h\alpha}{b_1} & 0 \\ \frac{1}{2} & -\frac{1}{2} & 0 & \frac{h\alpha}{b_2} \end{bmatrix}, \quad w = \begin{bmatrix} u_N \\ v_0 \\ (B_1 S u)_N \\ (B_2 S v)_0 \end{bmatrix}.$$

Obtaining an energy estimate requires

$$\tau \leq -\frac{b_1 + b_2}{4h\alpha}, \quad (3.18)$$

such that R becomes positive semi-definite. Here $b_{1,2}$ denotes the local values of $b_{1,2}$ at the interface.

4. 3-D simulations on unstructured grids

By combining symmetric second-derivative SBP operators and the SAT method, to implement the boundary conditions (see for example (3.9)), we obtain an ODE system (with N unknowns)

$$\begin{aligned} v_{tt} &= Qv + G(t) \\ v(0) &= f_1, v_t(0) = f_2 \end{aligned}, \quad (4.1)$$

for the discrete solution vector v . In Section 3 we have shown that the matrix Q have non-positive and real eigenvalues (a necessary stability condition) by utilizing the energy method. For the second-order accurate case we approximate v_{tt} using the central second-order scheme resulting in an explicit two-step method (see Mattsson & Nordström (2006) for details). The present method has been implemented for unstructured tetrahedral grids using a node-based finite-volume discretization.

4.1. Verification

In the first test we verify the accuracy and stability of the Dirichlet boundary conditions. The semi-discrete finite volume system, including Dirichlet boundary conditions, can be written:

$$\bar{H}Av_{tt} = (-\bar{M} + \bar{B}S_{i,b}) + \epsilon(\bar{B}S_{i,b})^T(v - g) + \sigma B_{i,b}(v - g), \quad (4.2)$$

where \bar{H} is the nodal volume, \bar{M} is the symmetric unstructured volume-integrated Laplacian operator described in Ham *et al.* (2006). Here $\bar{B}S_{i,b}$ is the volume-integrated gradient operator, which is based on Green-Gauss integration over the one-sided boundary nodal volumes assuming a linear variation in each associated tetrahedron. $B_{i,b}$ is the value of b at the boundary nodes. In the 1-D case we concluded (see Lemma 3.3) that σ is proportional to h^{-1} . Based on the previous structured 1-D analysis we expect that σ is proportional to $\bar{H}_{i,b}/A_{i,b}$, where $A_{i,b}$ is the area magnitude and $\bar{H}_{i,b}$ the nodal volume associated with the boundary node. The penalty parameters ϵ , σ in (4.2) are completely analogous to the ones in the 1-D case (3.9).

An energy estimate exists for the choice $\beta = 1$ and $\sigma = -\gamma\bar{H}_{i,b}/A_{i,b}$, for some γ large enough. Unlike the uniform structured 1-D case, it is more complicated to analytically derive a single sharp value for the minimum borrowing penalty, i.e., γ_{min} , that is applicable to all unstructured grids. Instead we performed a numerical study. There was a slight variation of the threshold value at which the simulations become unstable, although always close to 1, the limit in the 1-D case.

To verify the stability and accuracy of the unstructured implementation, a triply-periodic tetrahedral mesh was generated around a $2 \times 2 \times 2$ array of three cube compounds. Inspiration for this choice of geometry comes from M. C. Escher's Waterfall (see Fig. 1). Our cubes have a characteristic dimension of 0.2, and have center-to-center spacing of 0.5 in a $1 \times 1 \times 1$ box. The simulation of the wave equation in the surrounding volume requires an unstructured mesh to capture the complex polyhedral boundaries, although at any resolution the boundaries are precisely represented because all surfaces are planar. This allows us to generate a series of fine grids starting from a coarse grid by recursively applying a tetrahedral-splitting algorithm.

A grid convergence study was performed using the sequence of triply-periodic grids described previously and computing the standing wave problem $u = \sin(wct)\sin(wx)$, with the exact solution as initial condition and time-dependent Dirichlet boundary data. The convergence rate is calculated as

$$q = \log_{10} \left(\frac{\|u - v^{(N_1)}\|_h}{\|u - v^{(N_2)}\|_h} \right) / \log_{10} \left(\frac{N_1}{N_2} \right)^{1/d}, \quad (4.3)$$

where d is the dimension (here $d = 1$), u is the analytic solution, and $v^{(N_1)}$ the corresponding numerical solution with N_1 unknowns. $\|u - v^{(N_1)}\|_h$ is the discrete l_2 norm of the error. The results are presented in Table 1, where the grid sizes range from 46,680 tetrahedra up to 23,900,160 tetrahedra on the finest grid. With each grid refinement

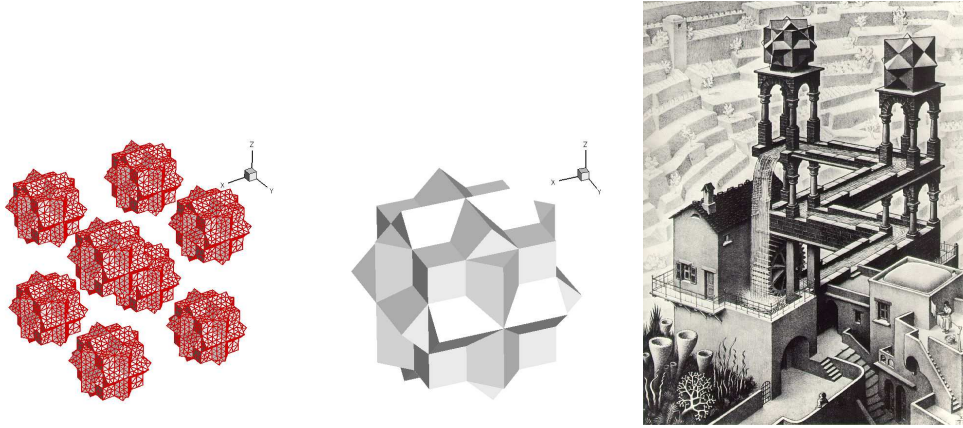


FIGURE 1. Geometrical details and inspiration for the three cube compounds.

N	$\log(l_2)$	q	Δx	$\log(l_2)$	q
46,680	-1.46	-	0.0625	-1.11	
373,440	-2.08	2.056	0.03125	-1.70	1.97
2,987,520	-2.69	2.028	0.015625	-2.31	2.07
23,900,160	-3.30	2.003	0.0078125	-2.92	2.04
			0.00390625	-3.52	2.00

TABLE 1. Unstructured grid refinement study: reduction in l_2 error with grid refinement for Dirichlet BC (left) and discontinuous interface (right).

the time step was also refined by a factor of 2 such that the temporal integration error remained small.

In the second test we verify the accuracy for the discontinuous interface. We chose an analytic solution

$$\begin{aligned} u &= \cos(w_1 c_1 t) \cos(w_1 x), & x \in [-1, 0], & t \geq 0, & w_1 = (2n + 1)\pi, & m, n \in \mathbf{Z} \\ v &= \cos(w_2 c_2 t) \cos(w_2 x), & x \in [0, 1], & t \geq 0, & w_2 = (2m + 1)\pi, & c_2 = c_1 \frac{w_1}{w_2}, \end{aligned}$$

and compute the solution on a square multi-block domain with $a_1 = b_1 = 1$, $a_2 = b_2 = 0.6$, $n = 1$ and $m = 2$. A convergence study is shown in Table 1.

4.2. Application

As a qualitative illustration of the method's capability, we compute the 3-D propagation of a Gaussian pulse in the volume surrounding the $2 \times 2 \times 2$ array of 3-cube compounds. For this case, we made use of the unstructured mesh to significantly extend the grid at modest cost to help reduce reflections at the far field boundary. The simulations reported below were run on the finest grid (see Table 1) produced by 3 applications of recursive tetrahedral refinement to this coarse grid.

To qualitatively investigate the effect of the Dirichlet boundary conditions, the same simulation was run with homogenous Neumann boundary conditions at the boundaries. Results from these simulations are compared in Fig. 2. The grid for this simulation

consisted of 31,126,528 tetrahedra, with constant computational time step $\Delta t = 0.00025$. Results are plotted on a plane passing through the center of 4 of the polyhedra for 3 times, $t = 0.25$, $t = 0.5$, and $t = 0.75$. The location of the center of the initial pulse is in this plane and displaced slightly toward the upper right, producing the observed diagonal symmetry. At $t = 0.75$ the coarseness of the outer grid (see Fig. 2) can be seen producing some reflections.

In the last computation we discretize the interior of the 3-cube compounds and use $a_1 = b_1 = 1$ on the outside domain and $a_2 = b_2 = .2$ on the inside. We then apply the discontinuous interface treatment to compute the 3-D propagation of the Gaussian pulse. The result from that simulation is presented in Figure 2.

5. Conclusions and future work

Time stable boundary treatments are derived for the wave equation on second-order form and on discontinuous media. We consider an unstructured Finite Volume discretization to handle complex geometries in 3-D. The methodology is based on the SBP properties of the schemes in combination with the SAT penalty technique to impose general boundary and interface conditions. The efficiency and accuracy of this method has been verified by numerical simulations.

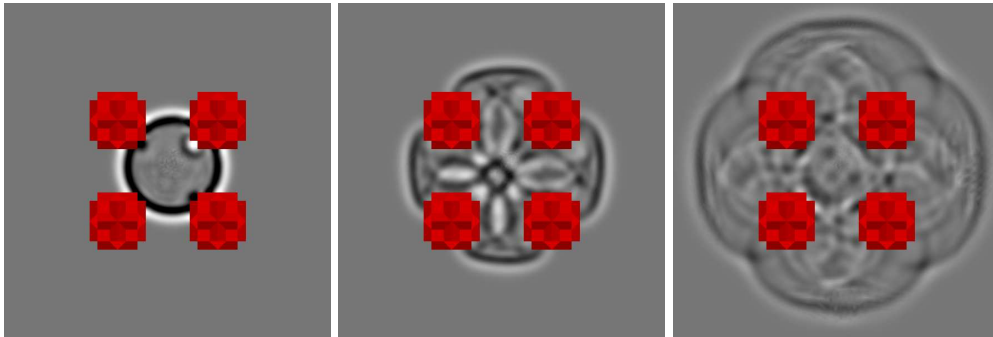
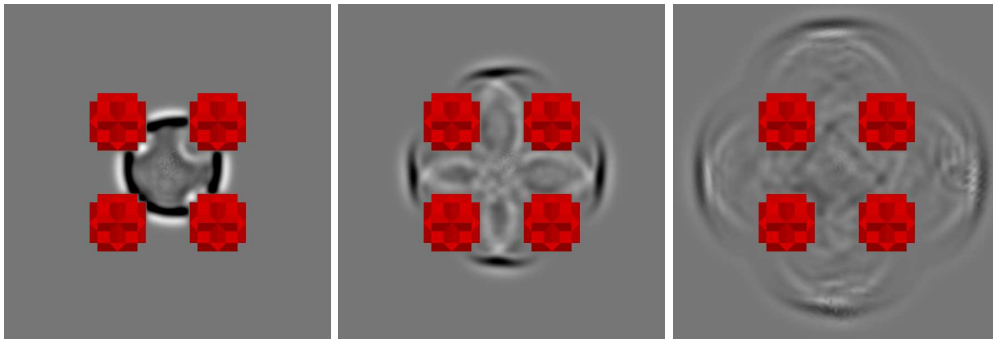
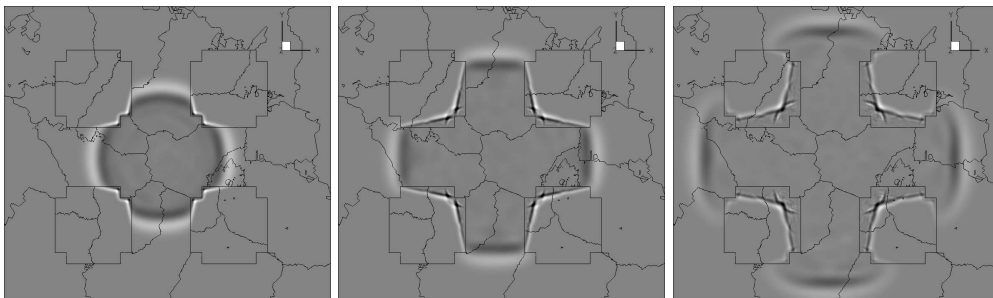
The next step will be to couple the unstructured finite volume discretization to a high order finite difference discretization to obtain an efficient hybrid method. That will also require some effort to handle the far field boundaries using non-reflecting boundary conditions.

Acknowledgments

This work is supported by the Advanced Simulation and Computing Program of the United States Department of Energy.

REFERENCES

- BAMBERGER, A. & GLOWINSKI, R. & TRAN, Q. H. 1997, A domain decomposition method for the acoustic wave equation with discontinuous coefficients and grid change. *SIAM J. Num. Anal.* **34**, 603–639.
- CARPENTER, M. H. & GOTTLIEB, D. & ABARBANEL, S. 1994, Time-stable boundary conditions for finite-difference schemes solving hyperbolic systems: Methodology and application to high-order compact schemes. *J. Comp. Phys.* **111**, 220–236.
- CARPENTER, M. H. & NORDSTRÖM, J. & GOTTLIEB, D. 1999, A Stable and Conservative Interface Treatment of Arbitrary Spatial Accuracy. *J. Comp. Phys.* **148**, 341–365.
- COHEN, G. & JOLY, P. 1996, Construction and analysis of fourth-order finite difference schemes for the acoustic wave equation in nonhomogeneous media. *SIAM J. Num. Anal.* **33**, 1266–1302.
- GUSTAFSSON, V. & MOSSBERG, E. 2004, Time compact high order difference methods for wave propagation. *SIAM J. Sci. Comput.* **26**, 259–271.
- GUSTAFSSON, V. & WAHLUND, P. 2004, Time compact difference methods for wave propagation in discontinuous media. *SIAM J. Sci. Comput.* **26**, 272–293.

(a) Neumann boundary conditions: $\partial\phi/\partial n = 0$ (b) Dirichlet boundary conditions: $\phi = 0$ 

(c) Discontinuous media.

FIGURE 2. Propagation of a 3D Gaussian pulse comparing different boundary and interface conditions on the $2 \times 2 \times 2$ array of 3-cube compounds.

HAGSTROM, T. 1999, Radiation boundary conditions for the numerical simulation of waves. *Acta Numerica* **8**, 47–106.

HAM, F. & MATTSSON, K. & IACCARINO, G. 2006 Accurate and stable finite vol-

ume operators for unstructured flow solvers *Center for Turbulence Research Annual Research Briefs* Stanford University, Stanford, California.

- KREISS, H.-O. & PETERSSON, N. A. & YSTRÖM, J. 2002, Difference approximations for the second order wave equation. *SIAM J. Num. Anal.* **40**, 1940–1967.
- KREISS, H.-O. & PETERSSON, N. A. & YSTRÖM, J. 2004, Difference approximations of the Neumann problem for the second order wave equation. *SIAM J. Num. Anal.* **42**, 1292–1323.
- KREISS, H.-O. & PETERSSON, N. A. 2006, A Second Order Accurate Embedded Boundary Method for the Wave Equation with Dirichlet Data. *SIAM J. Sci. Comput.* **27**, 1141–1167.
- MATTSSON, K. & NORDSTRÖM, J. 2004, Summation by parts operators for finite difference approximations of second derivatives. *J. Comp. Phys.* **218**, 503–540.
- MATTSSON, K. & NORDSTRÖM, J. 2006, High order finite difference methods for wave propagation in discontinuous media. *J. Comp. Phys.* **220**, 249–269.
- SHUBIN, G. R. & BELL, J. B. 1987, A modified equation approach to constructing fourth order methods for acoustic wave propagation. *SIAM J. Sci. Stat. Comput.* **8**, 135–151.
- SZILAGYL, B., & KREISS, H.-O. & WINICOUR, J. W. 2005, Modeling the Black Hole Excision Problem. *Physical Review D* **71**, 104035.
- TSYMKOV, S. V. 1998, Numerical solution of problems on unbounded domains. A review. *Applied Numerical Mathematics* **27**, 465–532.